*Korean J. Chem. Eng.*, 39(9), 2474-2481 (2022)
DOI: 10.1007/s11814-021-1049-0

pISSN: 0256-1115
eISSN: 1975-7220

# Effect of drainage layer on pressure drop of dual-layer glass fibrous coalescing filters

**Chengwei Xu*,†, Yan Yu**, and Xiaodong Si*****

*College of Electrical, Energy and Power Engineering, Yangzhou University, Yangzhou, 225127, China
**College of Engineering, Hebei Normal University, Shijiazhuang, 050024, China
***School of Energy and Power, Jiangsu University of Science and Technology, Zhenjiang 212003, China
(*Received 4 October 2021 • Revised 19 December 2021 • Accepted 22 December 2021*)

**Abstract**−Drainage layer strategy is a common method for improving the filtration performance of a coalescing filter. In this study, we employed commercial, sub-high efficiency glass fibrous filters as drainage layers. The performance of high efficiency coalescing filters assembling the drainage layer was investigated experimentally. After drainage layer was assembled, the wet pressure drop at equilibrium stage was reduced and the pressure drop allocation exhibited obvious change. In addition, the influence of pore size, thickness and wettability of drainage layer on performance was evaluated. The pore size is a dominant factor in improving wet pressure drop at steady state. The wet pressure drop reduces gradually over pore size. The drainage layer with smallest pore size shows highest quality factor. Likewise, the thickness of the drainage layer also has a positive effect on wet pressure drop and quality factor. The coalescing filter assembling thickest drainage layer has lowest pressure drop and highest quality factor. The effect of superoleophilic drainage layer on wet pressure drop and quality factor of filter is negligible, and the superoleophobic drainage layer results in the enhancement of pressure drop and reduction of quality factor. For different coalescing filters with the same drainage layer, the smaller the pore size deviation between coalescing and drainage layer, the lower the wet pressure drop and the higher the quality factor.

Keywords: Oil Particle, Drainage Layer, Pore Size, Filtration Performance, Coalescence, Pressure Drop

## INTRODUCTION

Oil particles in a gas stream are important pollutants generated from cooking activity and some industrial processes, such as natural gas transport, large rotating crankcase ventilation and compressed air system [1,2]. In China, cooking fume containing a large amount oil particles is directly or simply treated, then released to the atmosphere. The oil particles affect the air quality and harm human health [3]. In addition, oil particles existing in an process also cause serious problems, including indoor air contamination, machinery damage, corrosion and energy consumption [4-6].

Fibrous coalescence filtration is an effective and predominately used method for removing oil particles from a gas stream. Based on "coalesce mechanism," oil particles are intercepted onto the fibers, then coalescence and migration process assembling the filter. Wet pressure drop and quality factor are the key performance criteria of filters. Due to the mobility and redistribution of liquid, coalescence filtration is a complex dynamic process. Contal and Firsing et al. [7,8] divided the dynamic process into four stages according the change of pressure drop. They found that the accumulation of oil particles led to an exponential increase of pressure drop and the coalescing filter reached saturation state finally. The performance of coalescing filter is affected by fibrous material [9], fiber wettability [10], filter structure [11], liquid surface tension [12], pore size [13], and so on. Based on the fiber wettability, Penner et al. [14] conducted performance experiments of several configuration filters combining oleophilic and oleophobic media. They proposed two mechanisms for improving the performance by beneficial configuration. Wei et al. [15,16] designed many coalescing filters with asymmetric wettability structure. Those filters had higher quality factor compared with common homogeneous wettability filters. These studies were focused on filters with special wettability.

Apart from wettability, the drainage layer is another important strategy on improving filtration performance since it provides drainage channels and affects the wet pressure drop. The drainage layer was introduced into coalescing filter by multi-layered structure [17, 18]. Patel et al. [19] compared the performance of filters equipped with different orientation drainage layer. The result indicated that filters with a drainage layer showed higher quality factor. The low surface energy drainage layer had better coalescence performance [20]. Chang et al. [17,21] used different fibrous media filter as drainage layer to investigate the performance of coalescing filters. They found that the drainage layer leads to increase of liquid amount on the interface between the coalescing layer and drainage layer, which causes increase of pressure drop and saturation of filter. Most of these works, however, focus on orientation, fibrous material, and ordinary wettability. Many properties of drainage filter have a considerable impact on the coalescence performance of filter, such as pore size, the pore size deviation between coalescing and drainage layer, and super-wettability. The influence of those properties on performance needs to be studied further.

Glass fiber media is one of the most common commercial materials for coalescing filters owing to low cost, large surface face, high efficiency, ease of assembly and functionalization. Herein, we em-

†To whom correspondence should be addressed.
E-mail: xcwwfl1227@163.com

ployed glass fiber filters with different precision as coalescing layer and drainage layer. The effect of drainage layer on filter performance was investigated experimentally. In addition, we used glass fiber filters as substrate to fabricate superoleophobic and superoleophilic drainage layers. The change profile of pressure drop was analyzed by "jump-and-channel" model and capillarity in coalescing filter. The results provide further understanding of influence of the drainage layer on coalescence filtration performance.

## EXPERIMENTS

### 1. Materials

The filters used in this paper were built as "sandwiches" consisting of three layers glass fiber media. All test filter sheets were stacked to build the test sample. All filters were purchased from Zaisheng Technology Corp, Ltd. The glass fiber filters with four high efficiency grade (HEPA-H10, H11, H12 and H13) were used as coalescing layer. The coalescing layer was composed of 2-layer identical HEPA glass fiber filters. Drainage layer employed the glass fiber filter with large pore diameter and sub-high efficiency grade (ASHRAE-F6, F7, F8 and F9). The oil contact angle of original HEPA glass fiber was about 55°. According to the jump-and-channel model [22,23], a liquid film formed on the rear face of filter. Therefore, to get the most out of the drainage layer, it was assembled at the outlet side of the test filter. In addition, filters consisting of 2-layer HEPA filters were used as the control filter. All multilayer filters were constructed in triplicate. Table 1 lists the properties of original filter media.

The fiber diameter was calculated by Davies' equation:

$$\Delta P = \frac{64\mu U z \alpha^{1.5}}{d_f^2}(1+56\alpha^3) \quad (1)$$

where, $\Delta P$ is the pressure drop of clean filter, $\mu$ is the dynamic viscosity of air, U is the air velocity, z is the thickness of filter, $\alpha$ is the packing density of filter, $d_f$ is the fiber diameter.

Pore size of filters was measured by a pore size distribution analyzer (GaoQ, PSDA-20). Other parameters were provided by the manufacturer. Before usage, all test filters were treated in ethanol by ultrasonics to remove grease, then were washed repeatedly using distilled water and dried at room temperature.

The superoleophilic and superoleophobic paints were obtained from the School of Materials Science and Engineering, Southeast

**Table 1. Properties of original filters**

| Filter | category | Fiber diameter (μm) | Grammage (g/m$^2$) | Thickness (mm) | Packing density | Pore size (μm) |
|---|---|---|---|---|---|---|
| HEPA-H13 | Coalescing layer | 1.35 | 85.6 | 0.33 | 0.094 | 7.29 |
| HEPA-H12 | | 1.47 | 81.5 | 0.33 | 0.089 | 10.96 |
| HEPA-H11 | | 1.70 | 75.4 | 0.33 | 0.082 | 12.7 |
| HEPA-H10 | | 1.94 | 71.3 | 0.33 | 0.078 | 15.9 |
| ASHRAE-F9 | Drainage layer | 2.48 | 69.2 | 0.33 | 0.076 | 22.54 |
| ASHRAE-F8 | | 3.22 | 67.2 | 0.33 | 0.074 | 33.98 |
| ASHRAE-F7 | | 3.62 | 65.3 | 0.33 | 0.071 | 35.3 |
| ASHRAE-F6 | | 4.31 | 63.1 | 0.33 | 0.069 | 35.6 |

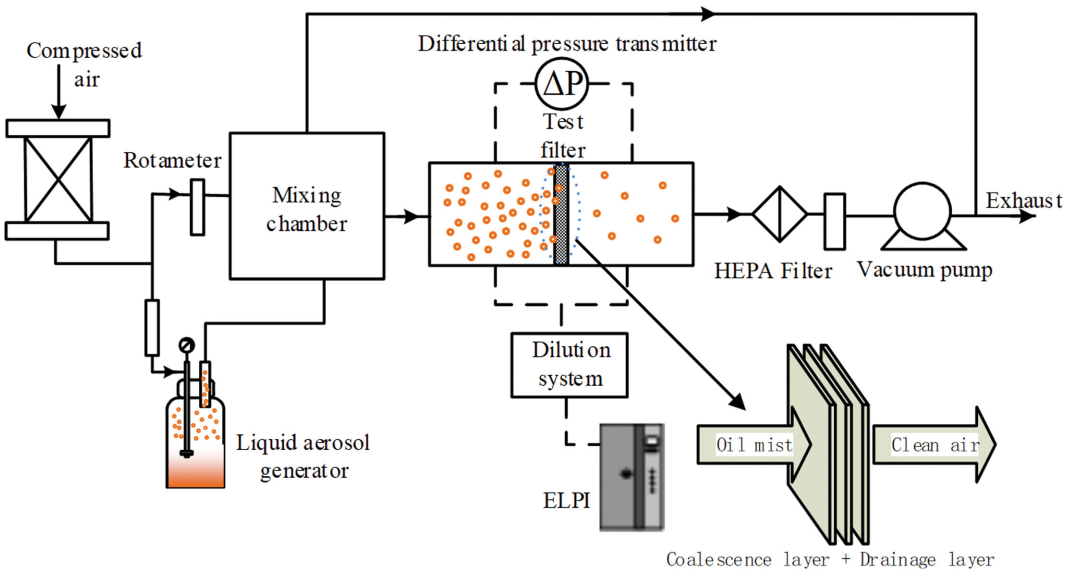


**Fig. 1. Experimental setup for filtration performance test.**

University; the detailed preparation procedure is described in Ref [24]. Briefly, after being washed and dried, the test drainage layer filters are separately dipped in superoleophilic and superoleophobic paints for 30 minutes to ensure all fibers are wetted completely. Then the wetted filters are taken out from the paints and dried at room temperature for 24 h. The superoleophilic and superoleophobic drainage layer sheets are obtained. The contact angle of oil on drainage layer filters is measured using a contact angle goniometer (Powereach® JC2000D).

**2. Experiment Setup**

Filtration performance tests were conducted on a special apparatus as shown in Fig. 1. Edible oil was selected as pollutant to generate oil mist and dispersed into a polydisperse population by a Laskin Nozzle atomizer manufactured in-house. The size distribution of particles from liquid aerosol generator is in the range of 40 nm-8 μm, and peak at 210 nm. Dried compressed air was applied as carrier gas and mixed gas. The test filters were placed into a filter holder. All coalescence tests were carried out at face velocity of 18 cm/s and loading rate of 165.6 mg/h. An electrical low pressure impactor (ELPI, Dekati) was used to measure the aerosol concentration and size distribution at upstream and downstream of test filters. The change of the pressure drop of test filters was continuously online recorded using a differential pressure transmitter (Asmik, MIK-9600D). The experiments were repeated three times.

After each experiment was finished, the test filter was dismantled from the filter holder and disassembled to several sheets. The oil content of each sheet was weighed by an electronic balance. The saturation (S) of each sheet can be calculated as:

$$S = \frac{m_{oil}}{m_{oil,\,void}} = \frac{m_s - m_0}{V\rho_{oil}(1-\alpha)} \quad (2)$$

where, $m_{oil}$ is the mass of oil captured in the filter, $m_{oil,\,void}$ is the maximum oil content of the filter, V is the total volume of filter, $\rho_{oil}$ is the density of edible oil, $m_s$ is the mass of the saturated filter sheet and $m_0$ is the mass of the clean filter sheet.

## RESULTS AND DISCUSSION

**1. Effect of the Drainage Layer on Coalescence Performance**

The dynamic pressure drop can be generalized to three or four stages owing to oil droplet migration and aggregation [7,8]. However, as shown in Fig. 2(a), the pressure drop profiles of two layers glass filter cannot be divided into three or four stages. It is because the filters only are stacked without compaction and there are air gaps between filter layers. To illustrate the pressure drop evolution accurately, the jump-and-channel model [22,23] was employed to analyze the wet pressure drop. According to the model, the wet pressure drop consists of jump and channel pressure drop. The jump pressure drop is required to overcome the capillary force for exiting or entering the filter, and the channel pressure drop reflects the liquid transport inside the filter. Fig. 2(a) shows the pressure drop curve over time. There are two channel and jump regions for a dual-layer filter. The liquid was transported through the first layer media and formed many liquid channels. Those liquid channels took 11 min to reach stable state, as shown in Channel region in Fig. 2(a). The flow resistance from liquid channels was 2.13 kPa. Then, liquid gradually coalesced, redistributed and formed liquid film to cover the rear face of the first layer media. Liquid films at air gaps generated the jump pressure drop (5.55 kPa). Partial liquid was sucked into the second layer and generated the channel and jump pressure drop in second layer filter.

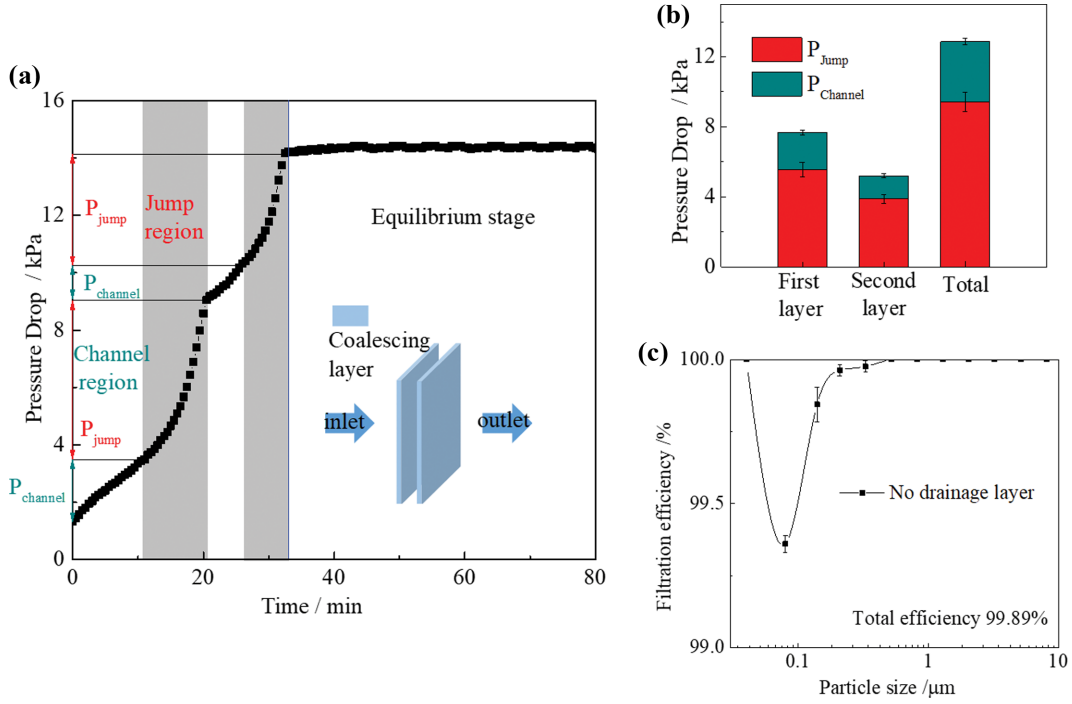


**Fig. 2. Pressure drop evolution and filtration efficiency of 2 layers HEPA-H13 filter without drainage layer, (a) pressure drop profile versus time; (b) channel and jump pressure drop of filter media; (c) filtration efficiency of different size particles at equilibrium stage.**

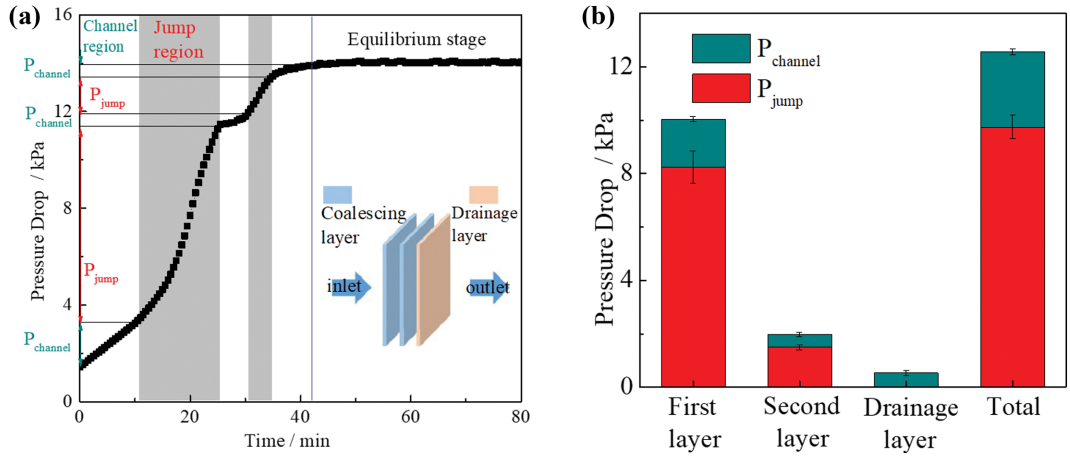


**Fig. 3. Pressure drop evolution and filtration efficiency of 2 layers HEPA-H13 filter with drainage layer (ASHRAE-F6), (a) pressure drop profile versus time; (b) channel and jump pressure drop of filter media.**

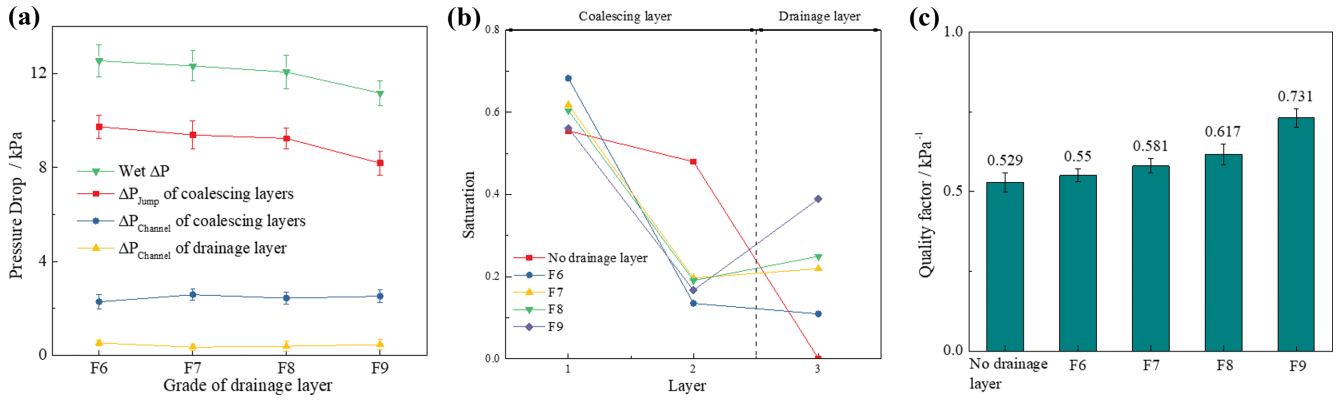


**Fig. 4. Performance of filter with different drainage layers at equilibrium state, (a) pressure drop, (b) saturation, (c) quality factor.**

Fig. 2(b) shows the pressure drop of each layer filter. Note that the channel and jump pressure drop of second layer media is less than that of first layer. Because the first layer has a high efficiency (>99.97%) in capturing liquid aerosols, the second layer was not loaded via aerosol transport but by capillary transport from the air gap. In addition, higher value of jump pressure drop represents greater amount of liquid film [17]. The result shows that the amount of liquid at interface is more than at rear face of second layer. The filtration efficiency of different size particles is shown in Fig. 2(c). The total number efficiency is 99.89%. It is attributed to the high filtration grade of each media (HEPA). The efficiency at 0.08 nm is only 99.25%.

When assembling the ASHRAE-F6 drainage layer outside of the coalescing layer, the pressure drop evolution in time changed, as shown in Fig. 3(a). Compared with the filter without drainage layer, the most signification difference is the wet pressure drop proportion of each layer filter. The pressure drop of first layer increased from 7.68 to 10.04 kPa and that of second layer decreased from 5.19 to 1.98 kPa. In addition, the drainage layer only generates the channel pressure drop (0.53 kPa), which results in trifling increase of total wet pressure drop.

Fig. 3(b) shows that jump pressure drop value of first layer is higher than second layer, due to the increase of the saturation of first layer. The high jump pressure drop of first layer suggests that the area and amount of liquid film increased between the coalescing layers. It is difficult to observe the distribution and change of liquid film on the rear face of first layer because capillarity causes redistribution of the liquid once the air flow is shut off. The change of pressure drop of first layer is derived from the saturation, as shown in Fig. 4(b). It can be seen that the saturation of first layer increases differently due to equipping different drainage layer. Furthermore, the lower jump pressure drop of second layer indicates that the drainage layer can reduce the accumulation of liquid on the rear face of the adjacent layer. The evolution of jump pressure drop indicates that the drainage layer caused the redistribution of liquid film in coalescing layers.

The channel pressure drop of first layer does not obviously change in all cases without drainage layer. And the channel pressure drop of second layer decreases from 1.31 to 0.48 kPa as equipping the drainage layer. It is attributed to the decrease of liquid holding volume of second layer and the amount of liquid channel. On the other hand, the total wet pressure drop of the filter with drainage layer reduces 0.32 kPa. It shows that the wet pressure drop of filter can be improved slightly by being equipped with a drainage layer.

## 2. Effect of the Properties of the Drainage Layer on Coalescence Performance

Pore size of drainage layer is an important parameter which affects the performance of the coalescing filter. To investigate the effect of pore size of drainage layer, four different filters (ASHRAE-F6, F7, F8 and F9) were employed as the drainage layer. The pore size of the drainage layer ranges from 35.6 to 22.54 μm, as shown in Table 1. Fig. 4(a) shows the wet channel and jump pressure drop of the coalescing filter. The wet pressure drop of the filter decreases with the decrease in pore size. The reason for reduction of wet pressure drop is that the decrease of pore size results in the increase of capillary force. The capillary pressure is inversely proportional to the capillary radius according to Laplace's equation. Mullins et al. [25] analyzed the coalescence process of oleophilic fibrous filter media and developed a relationship between the capillary radius and the properties parameters of filter:

$$r_c = \left(-A\log_e\left(\frac{\alpha}{r_f}\right) - B\right)c_f \tag{3}$$

where, $r_c$ is the capillary radius, $r_f$ is the fiber radius, A and B are the media-specific constants, $c_f$ is the correlation coefficient.

According to Eq. (3), the smaller capillary radius of drainage layer is caused by the smaller pore size. Thus, the capillary force of drainage layer increases with the decrease of pore size. More liquid collected by the coalescing layer is dragged into the drainage layer, which results in the reduction of wet drop of coalescing layer as shown in Fig. 4(a). Theoretically, the jump pressure drop is only affected by the fibrous media properties, rather than the other operating parameters [22,23]. Thus, the jump pressure drop of coalescing filter should remain constant after assembling the drainage layer. However, it can be seen that the evolution of the jump pressure drop is in agreement with the wet pressure drop. It could be assumed that the jump pressure drop is the resistance of airflow essentially and directly related to the amount of oil film on the rear face of coalescing filter. This is visual evidence for the reduction of oil film on the coalescing layers caused by the decrease of pore size of drainage layer. Nevertheless, there is no direct correlation between channel pressure drop and pore size of drainage layer due to the small deviation of channel pressure drop in Fig. 4(a).

The saturation change of filter with different pore size drainage layer is shown in Fig. 4(b). The saturation of the first layer increases and that of second layer decreases sharply. The saturation change of coalescing layer is in agreement with the wet pressure drop in Fig. 2(b) and 3(b). In addition, the saturation of drainage layer increases with the reduction of pore size. To illustrate the correlation between the pore size and saturation, based on the modified Washburn equation, the equilibrium capillary rise height $x_\infty$ is calculated by

$$x_\infty = \frac{CT\cos\theta}{A_c\rho g} \tag{4}$$

where, C is the wetted perimeter of capillary, T is the surface tension of oil, $\theta$ is the contact angle, $\rho$ is the density of oil, g is acceleration due to gravity.

According to Eqs. (3)-(4), the capillary height of liquid at saturation state rises with the decrease of pore size and more liquid remains in the fibrous media. Thus, the saturation of the drainage layer is inversely proportional to pore size of drainage layer. The smaller the drainage layer pore size, the higher the saturation is. Moreover, there is no great difference between the second layer saturations with various drainage layers. The increment of liquid in drainage layer is mainly from the first layer. Thus, the saturation of first layer decreases as the pore size of drainage layer decreases. The smaller pore size of drainage layer results in stronger capillarity, more liquid is absorbed into the drainage layer. This is consistent with the results in previous study [17].

The quality factor $Q_f$ is generally used as the criterion to estimate filter performance, which is defined as:

$$Q_f = \frac{-\ln(1-E)}{\Delta P}$$

where, E is the filtration efficiency and ΔP is the wet pressure drop.

Fig. 4(c) shows the quality factor of filters with different drainage layers. The coalescing layer with drainage layer (F9) shows the highest quality factor. It is reasonable to conclude that the drainage layer strategy could effectively improve the filtration performance of coalescing filter.

Thickness is another characteristic parameter of drainage layer. The initial dry pressure drop of drainage layer is only 0.067 kPa at

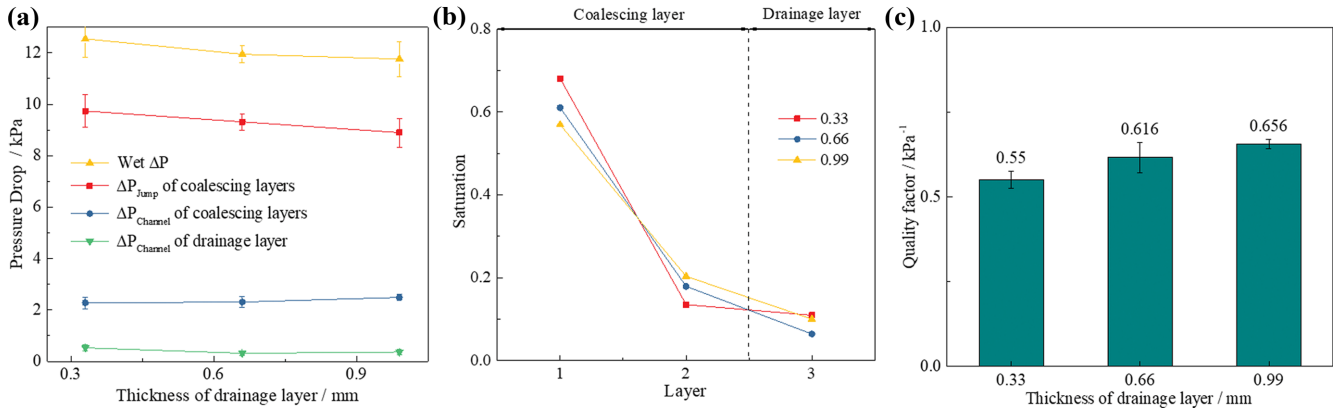


**Fig. 5. Performance of filter with different thickness of drainage layers at equilibrium state, (a) pressure drop, (b) saturation, (c) quality factor.**

face velocity 18 cm/s, which is further lower than the initial dry pressure drop of coalescing layer (1.33 kPa). Though the dry pressure drop is proportional to thickness, the effect of increasing thickness of drainage layer on dry pressure drop may be neglected. In this paper, the thickness of drainage can be varied by changing the number of layers.

Fig. 5(a) shows that the wet pressure drop is plotted against the thickness of drainage layer. Similarly, the jump pressure drop decreases in the increase of thickness of drainage layer. As shown in Fig. 5(b), the saturation of first layer is close to second layer when the thickness increases. According to capillary pumping model of porous media [25], the thicker drainage layer pumped more liquid into the drainage layer. The actual holding volume of drainage layer enhances. However, because the void volume of drainage layers multiplied, the apparent saturation of drainage layer shows a reduction tendency. The quality factor can be calculated by the efficiency and wet pressure drop, as shown in Fig. 5(c). The filter with the thickest drainage layer exhibited the best filtration performance. The results show that the coalescence performance can be improved by increasing the thickness of drainage layer.

The effect of wettability of drainage layer was studied by using three different surface property materials having untreated, superoleophilic and superoleophobic glass fiber media. The oil contact angle of original glass fiber filter is 62° and changes to 6.5° after oleophilic treatment. The oil contact angle of superoleophobic filters is 151.3°. Fig. 6(a)-(b) show the photograph of oil droplet on treated glass fiber filter.

While the contact angle of drainage layer changes from 62° to 6.5°, the jump pressure drop of coalescing layer reduces and the channel pressure drop increases, as shown in Fig. 6(c). According to the results in Fig. 6(d)-(e), the difference value of saturation between first layer and second coalescing layer decreases. This is because the liquid in drainage layer is hard to drain due to the excellent lipophilicity. The increase of saturation of drainage layer indicates that more liquid is sucked into the drainage layer. In addition, the wet pressure drop and quality factor of superoleophilic drainage layer is close to that of untreated drainage layer. Thus, the effect of contact angle on filtration performance could be neglected as filter is oleophilic.

When the drainage layer is superoleophobic, the wet pressure

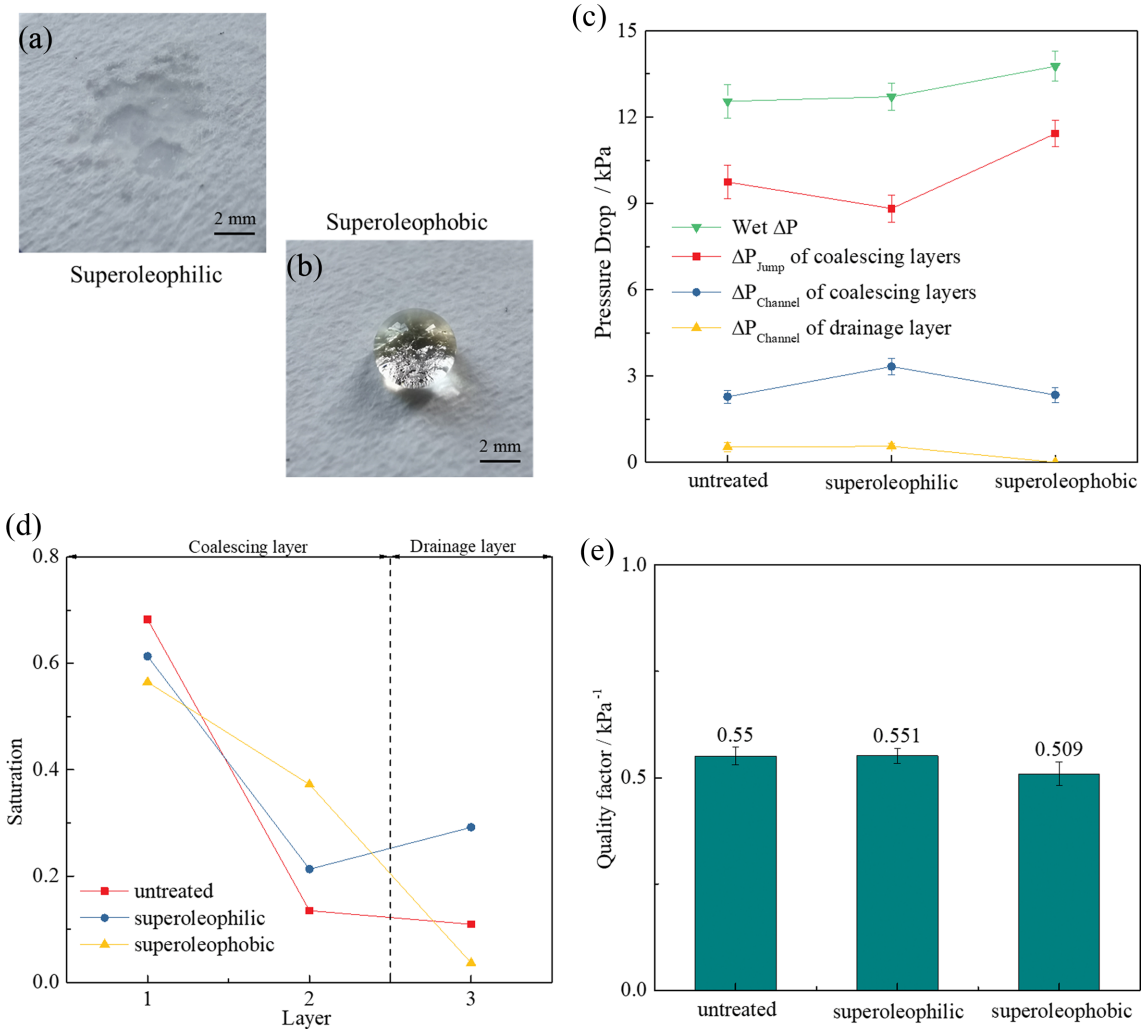


**Fig. 6. (a)-(b) photograph of edible oil on superoleophilic and superoleophobic drainage layer, (c) pressure drop of filters, (d) saturation profiles of layers, (e) quality factor of filters at equilibrium state.**

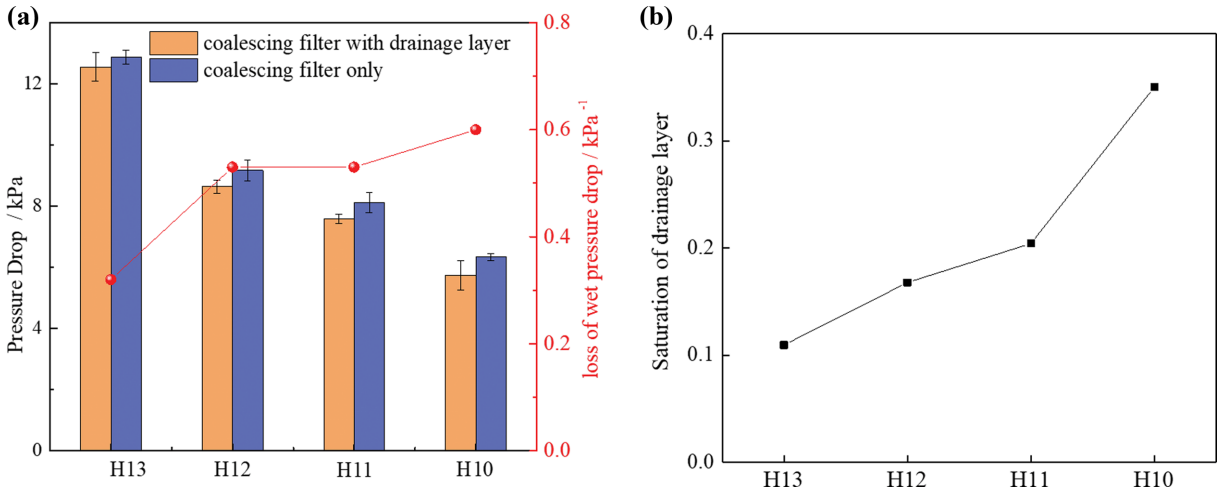


**Fig. 7. Variation of different coalescence filter with F6 drainage layer at steady state, (a) wet pressure, (b) saturation of drainage layer.**

drop and jump pressure drop of filter increase, as shown in Fig. 6(c). The increment of saturation of second coalescing layer is higher than decrement of first layer, which represents the increase of liquid amount on coalescing layer. The increase of jump pressure drop and saturation of second layer suggest that the liquid film on rear face of second layer increases. The reason for this result may be that the liquid on rear face of second layer aggregates largely because of the repellency of superoleophobic drainage layer and cannot be drained out in time. The quality factor of filter with superoleophobic drainage layer is 0.509 kPa$^{-1}$ and lower than other filters. It is obvious that the wettability of the drainage layer has slight influence on the filtration performance.

### 3. Effect of the Drainage Layer on Different Coalescing Filter

In practice, the different coalescing filters are selected to fit the various filtration requirements. Thus, the experiments were conducted to investigate the effect of drainage layer on different coalescing filter HEPA-H13, H12, H11, H10. The variation of wet pressure drop and saturation is shown in Fig. 7.

As equipping ASHRAE-F6 drainage layer, the wet pressure drop of all test filters was reduced and the decrement of wet pressure drop increased with the decrease of filter classification at steady state. The gravitational force affects the drainage rate vertically and cannot be discussed here. In this paper, the effect of drainage layer is mainly reflected on the liquid transport horizontally. A force balance of liquid film between the coalescing layer and drainage layer includes airflow force, drag force from coalescing layer, and suction force from drainage layer.

Due to the same drainage layer, the capillary suction force generated by drainage layer should be constant. However, the capillary drag force from coalescing layer decreases in the increase of the pore size of coalescing layer and the airflow force remains constant. Thus, more liquid is transported into the drainage layer. It can be verified by the data shown in Fig. 7(b). The saturation of ASHRAE-F6 drainage layer increases with the reduction of pore size of coalescing layer. The result also indicates that the smaller deviation of pore size of adjacent layers is more favorable to liquid transport.

As expected, the HEPA-H10 coalescing filter with ASHRAE-F6 drainage layer shows the highest quality factor and best filtration performance, as shown in Fig. 8. In addition, the increase rate of quality factor of HEPA-H10 is 19%, which is higher than other filters. The increase rate of quality factor gradually increases with the reduction of filter classification. This result shows that the impact of drainage layer method on diverse coalescing filters is different and the drainage strategy can improve the filtration performance of coalescing filters.

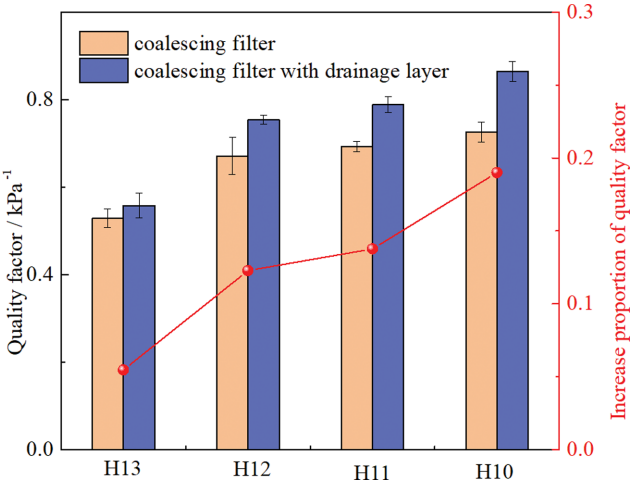


**Fig. 8. Quality factor of different coalescence filter with F6 drainage layer at steady state.**

## CONCLUSIONS

Experiments were conducted to investigate the effect of pore size, thickness and wettability of a series of sub-high efficiency drainage layers (ASHRAE-F6, F7, F8, F9) on high efficiency coalescing filters (HEPA-H10, H11, H12, H13). While the drainage layer was assembled, the total wet pressure drop reduced 0.32 kPa. The pressure drop of first layer increased from 7.68 to 10.04 kPa and that of second layer decreased from 5.19 to 1.98 kPa. The jump pressure drop of second coalescing layer significantly decreased and

that of first layer increased. The results indicate that the drainage layer causes the redistribution of oil in coalescence layers and promotes the drainage of the adjacent coalescence layer.

In addition, the smaller pore size of the drainage layer results in a lower wet pressure drop and higher quality factor. The drainage layer with smallest pore size (22.54 μm) shows the highest quality factor. The thickness of the drainage layer also affects the filtration performance. As increasing the thickness of drainage layer, the wet pressure drop of filter decreases and the quality factor increases. Furthermore, the superoleophilic and superoleophobic drainage layers were prepared as the control filters to explore the effect of wettability. It can be found that wettability can impact the oil distribution and transport on coalescence layer, but weakly affect the filtration performance. Moreover, four high efficiency coalescing filters with the same drainage layer exhibited different influence on wet pressure drop and quality factor. In particular, when the difference of pore size between the coalescing and drainage layers decreases, the improvement in the filtration performance is obvious.

## ACKNOWLEDGEMENTS

This work was supported by the National Natural Science Foundation of China (Grant No. 52100131) and the Natural Science Foundation of the Jiangsu Higher Education Institutions of China (Grant No. 20KJB470007).

## REFERENCES

1. X. Zhao, Q. Hu, X. Wang, X. Ding, Q. He, Z. Zhang, R. Shen, S. Lu, T. Liu, X. Fu and L. Chen, *J. Atmos. Chem*., **72**, 1 (2015).
2. R. Mead-Hunter, A. J. C. King and B. J. Mullins, *Sep. Purif. Technol*., **133**, 484 (2014).
3. C. Metayer, Z. Wang, R. A. Kleinerman, L. Wang, A. V. Brenner, H. Cui, J. Cao and J. H. Lubin, *Lung Cancer*, **35**, 111 (2002).
4. J. H. Lee, I. Kim, H. Seok, I. Park, J. Hwang, J. O. Park, J. U. Won and J. Roh, *Ann. Occup. Environ. Me.*, **27**, 19 (2015).
5. G. Gonfa, M. A. Bustam, A. M. Sharif, N. Mohamad and S. Ullah, *J. Nat. Gas Sci. Eng*., **27**, 1141 (2015).
6. J. S. Stahley, *Dry gas seals handbook*, PennWell Corp, Tulsa (2005).
7. P. Contal, J. Simao, D. Thomas, T. Frising, S. Calle, J. C. Appert-Collin and D. Bemer, *J. Aerosol Sci*., **35**, 263 (2004).
8. T. Frising, D. Thomas, D. Bémer and P. Contal, *Chem. Eng. Sci*., **60**, 2751 (2005).
9. G. M. Manzo, Y. Wu, G. G. Chase and A. Goux, *Sep. Purif. Technol*., **162**, 14 (2016).
10. B. J. Mullins, R. Mead-Hunter, R. N. Pitta, G. Kasper and W. Heikamp, *AIChE J*., **60**, 2976 (2014).
11. T. Jankowski, *Fibres. Text. East. Eur.*, **20**, 105 (2012).
12. F. Chen, Z. Ji and Q. Qi, *Sep. Purif. Technol*., **209**, 881 (2019).
13. F. Chen, Z. Ji and Q. Qi, *Sep. Purif. Technol*., **201**, 71 (2018).
14. T. Penner, J. Meyer and A. Dittler, *Sep. Purif. Technol*., **261**, 118255 (2021).
15. X. Wei, Y. Liu, H. Zhou, F. Chen, H. Wang, Z. Ji, G. G. Chase and T. Lin, *ACS Appl. Mater. Interfaces*, **12**, 28852 (2020).
16. X. Wei, H. Zhou, F. Chen, H. Wang, Z. Ji and T. Lin, *Adv. Funct. Mater*., **29**, 1806302 (2019).
17. C. Chang, Z. Ji and F. Zeng, *Sep. Purif. Technol*., **170**, 370 (2016).
18. Z. Liu, Z. Ji, J. Shang, H. Chen, Y. Liu and R. Wang, *Sep. Purif. Technol*., **198**, 155 (2018).
19. S. U. Patel and G. G. Chase, *Sep. Purif. Technol*., **75**, 392 (2010).
20. S. U. Patel, P. S. Kulkarni, S. U. Patel and G. G. Chase, *Sep. Purif. Technol*., **87**, 54 (2012).
21. C. Chang, Z. Ji and J. Liu, *Chem. Eng. Sci*., **160**, 354 (2017).
22. D. Kampa, S. Wurster, J. Buzengeiger, J. Meyer and G. Kasper, *Int. J. Multiphase Flow*, **58**, 313 (2014).
23. D. Kampa, S. Wurster, J. Meyer and G. Kasper, *Chem. Eng. Sci*., **122**, 150 (2015).
24. Z. Xiao, H. Zhu, S. Wang, W. Dai, W. Luo, X. Yu and Y. Zhang, *Adv. Mater. Interfaces*, **7**, 2070041 (2020).
25. R. Mead-Hunter, R. D. Braddock, D. Kampa, N. Merkel, G. Kasper and B. J. Mullins, *Sep. Purif. Technol*., **104**, 121 (2013).